Impact of Sterilization on the Adhesion Properties of a Polyamide 11 Coating on Textured Metal Substrates

Célia Badji, Ahmed Allal, Jean-Charles Dupin, Frédéric Léonardi

coatings

MDPI

Article

Impact of Sterilization on the Adhesion Properties of a Polyamide 11 Coating on Textured Metal Substrates

Célia Badji, Ahmed Allal, Jean-Charles Dupin and Frédéric Léonardi *

IPREM, E2S UPPA, CNRS, Université de Pau et des Pays de l'Adour, Technopole Hélioparc, 2 Avenue du Président Pierre Angot, 64053 Pau Cedex 09, France; celiabadji@gmail.com (C.B.); ahmed.allal@univ-pau.fr (A.A.); jean-charles.dupin@univ-pau.fr (J.-C.D.)

* Correspondence: frederic.leonardi@univ-pau.fr

Abstract: Polyamide materials are widely used for medical device coating. However, despite the fragile area at the interface, these devices must conserve their physical and mechanical performance after the sterilization process. In this work, the impact of steam sterilization, widely used in the medical sector, on the adhesion properties of biocompatible and biosourced polyamide-11-coated copper substrates was assessed. The adhesion strength, a quantitative indicator of the coating performance, was assessed thanks to a laboratory-made bench test. The surface of metal substrates was microstructured with laser engraving to enhance the coating adhesion. The Ra roughness value was varied to verify if the depth of valleys induced with the femtosecond laser could favor the interfacial anchoring. Scanning electron microscopy analyses highlighted the physical surface evolution of the polymer analyzed at the interface, across the various texturing parameter values, Ra. Fourier transform infrared spectroscopy was used to monitor the bands specific to polyamide thermo-oxidative degradation. Elemental composition deduced from X-ray photoelectron spectroscopy carried out on the coating after mechanical debonding clearly revealed that the chemical stability of the copper substrates was affected rather than the polyamide coating. Also, we discussed the impact of the chosen sterilization parameters (steam and pressure) on the formation of copper-based species detected with this technique.

Keywords: steam sterilization; polyamide; texturing; adhesion; fluidized bed

Citation: Badji, C.; Allal, A.; Dupin, J.-C.; Léonardi, F. Impact of Sterilization on the Adhesion Properties of a Polyamide 11 Coating on Textured Metal Substrates. *Coatings* **2024**, *14*, 424. https://doi.org/10.3390/coatings14040424

Academic Editors: Egemen Avcu, Yasemin Yıldıran Avcu and Mert Guney

Received: 13 February 2024
Revised: 28 March 2024
Accepted: 29 March 2024
Published: 31 March 2024

1. Introduction

The demand for safe and effective materials is greatly increasing in biomedical engineering due to the annual increase of the world's population, ageing of the European population, and the high functional demands of people. The fundamental requirement of a medical device is that the material and the surrounding should coexist without having any undesirable effect one on another. Tools for invasive procedures or patient care made from polymer-based materials are indispensable helpers in many fields of modern medicine. Companies have recently developed solutions to replace existing hard instruments with softer surgical instruments whose functions can be filled with polymer-based materials [1]. For instance, tools like metal retractors for heart surgery can be coated with a biosourced thermoplastic coating to protect the metal dispositive and avoid some injuries to the patient [2]. Polyamides are biobased conventional polymers [3] that are often used for the coating of retractors for skin or tissue spacing [1] due to their flexible nature, effectiveness and affordability [1,2]. However, they must undergo a conformity assessment and comply with regulations [4,5]. These evaluations include, inter alia, the test of the mechanical performance of the polymer-based medical device, like fatigue or shear testing, depending on its service life [6].

Proper sterilization strongly influences the overall success of the intervention and ensures the safety of both the patient and medical personnel. In this aim, thermoplastics and resins need an extended, critical evaluation in terms of potential sterilization methods

to highlight the effects of sterilization on the mechanical parameters and internal structure of the final product. Nylons are known to be biocompatible and withstand the sterilization cycles without causing any defect on their properties. Autoclaving is typically used by medical tools developers (companies) and users (hospitals) following the recommendations of the health authorities [7]. Wingham et al. studied the effect of steam autoclaving on mechanical properties of polyamide 12 (PA12) [8]. Their work reveals that changes in mechanical properties were observed after steam sterilization. Nevertheless, these changes were correlated with the water uptake, suggesting that an oven-drying step is mandatory after the sterilization treatment. Indeed, original properties were reobtained after drying of the samples [8]. Also, Told et al. carried out sterilization of PA12 material through several sterilization techniques including autoclaving, after 10 or 20 cycles [9]. Even if the impact strength decreased in all cases, the largest decrease occurred after 20 cycles of autoclave sterilization. Despite these variations in mechanical properties, no change in the cross section measured with a caliper was observed. However, no study on single-use devices that only need one cycle of sterilization, like those presented in our study, has been reported. We could expect that this device presents a different performance. Otherwise, to our knowledge, there is no information in the literature about the resistance to sterilization of polyamide-11 (PA11)-coated metal devices.

Various texturing processes such as laser surface texturing (LST), electric discharge texturing, focused ion beams, abrasive blasting and lithography have been employed by researchers for biomedical applications [10–12]. LST is typically and widely used to generate micropatterns. It has recently shown tremendous potential in biomedical applications [13] due to its high-efficiency, excellent controllability, environmental friendliness and accuracy. Investigations involving the LST were conducted on metals like zirconia for dental implants to enhance hydroxyapatite adhesion on the zirconia surface [14], of steel for microfluidic applications [15] or of copper to favor its bactericidal properties [16]. Also, in the study conducted by Razzaq et al., the copper metal was treated with LST to enhance corrosion resistance and improve its surface properties [17]. Results showed that laser irradiation enhanced the corrosion resistance of the metal copper linked to the grain refinement of the surface layer. The effects of periodic surface structuring of copper thanks to an ultrafast laser. The effects of LST on the wettability were also investigated by Long et al. [18]. The results evidenced that the subsequent wettability conversion was caused by the absorption of organic matter from the surrounding atmosphere. In addition, Conradi et al. observed that the corrosion of epoxy-coated steel surfaces induced by the ageing process was limited with LST [19]. Our study will complete the existent knowledge reported in the literature by providing insights on the effects of the metal substrates' structuring on the adhesion of a biocompatible thermoplastic coating before and after the sterilization process.

In our previous work dealing with a polyamide 11 coating on copper substrates processed with conventional fluidized bed coating, we observed that other parameters like preheating temperature and time of immersion in the fluidized bed could influence the coating properties [20]. It was observed that, even if increasing the copper preheating temperature promoted the aspect and thickened the coating, it undermined the interfacial adhesion. The main objective of this work is to evaluate the effects of steam sterilization on polyamide-coated copper samples. Our additional goal is to verify if the preliminary texturing of the metal support can help maintain the adhesion performance of the dispositive. Chemical and morphological analyses with spectrometry and microscopy measurements at the polyamide/copper interface were conducted to understand the mechanical performance changes of adhesion.

2. Material and Methods

2.1. Material

Polyamide 11 powder (PA11) was supplied by Arkema (Serquigny, France). Rilsan Invent Natural grade was used for metal coatings for its biocompatibilty (United States Pharmacopia (USP) class VI). Copper cylinders (diameter of 4.715 mm) supplied from

Goodfellow (Lille, France) were employed as a metal support. Copper has been chosen as the metal substrate for its high flexibility, a property that can be required for surgical interventions requiring surgical tools that can be adapted to the operation area [21]. Acetone (Sigma Aldrich, purity of ≥99.5%) and acetic acid (Sigma Aldrich, purity of ≥99%) were employed before the coating process to remove eventual organic pollutants and native oxide layers, respectively, from the metal substrates that could prevent efficient metal coating.

2.2. Laser Texturing of the Copper Surface

The surface treatment enabled an increase in the roughness of the copper substrate before the coating process was microprocessed by the technological center for optics and lasers, Alphanov (Bordeaux, France). An ultrafast fiber laser system (Tangerine HP, Amplitude Systems) emitting in the near infrared (central wavelength λ = 1030 nm) with an average power of 42 W and delivering ultrashort pulses whose width was between 0.35 ps and 10 ps was utilized for the texturing experiments. The average energy per pulse was indicated at 225 µJ and the maximum repetition rate was 40 MHz. The microprocessing was carried out longitudinally (Figure 1). A TR200 surface roughness tester was used to measure the average arithmetic roughness, Ra (µm). It is equipped with a standard sensor, TS-100 (Checkline Europe, The Netherlands), with a 5 µm diamond tip with 0.001 µm accuracy. The measurement interval ranges from 0.001 µm to 40 µm. According to ISO 4287 [22], Ra is the average of how far each point on the surface deviates in height from the mean height:

$$Ra\ (\mathrm{mm}) = \frac{1}{n}\sum_{i=1}^{n}|Zi| \quad (1)$$

where Zi is the vertical deviation according to the mean line (peaks and valleys) in µm and n is the number of points along the analysed axis. To obtain 3 different roughness values, these were gradually increased from 0.5 to 10 µm thanks to the increasing number of passages of the beam on the copper sample (see Table 1).

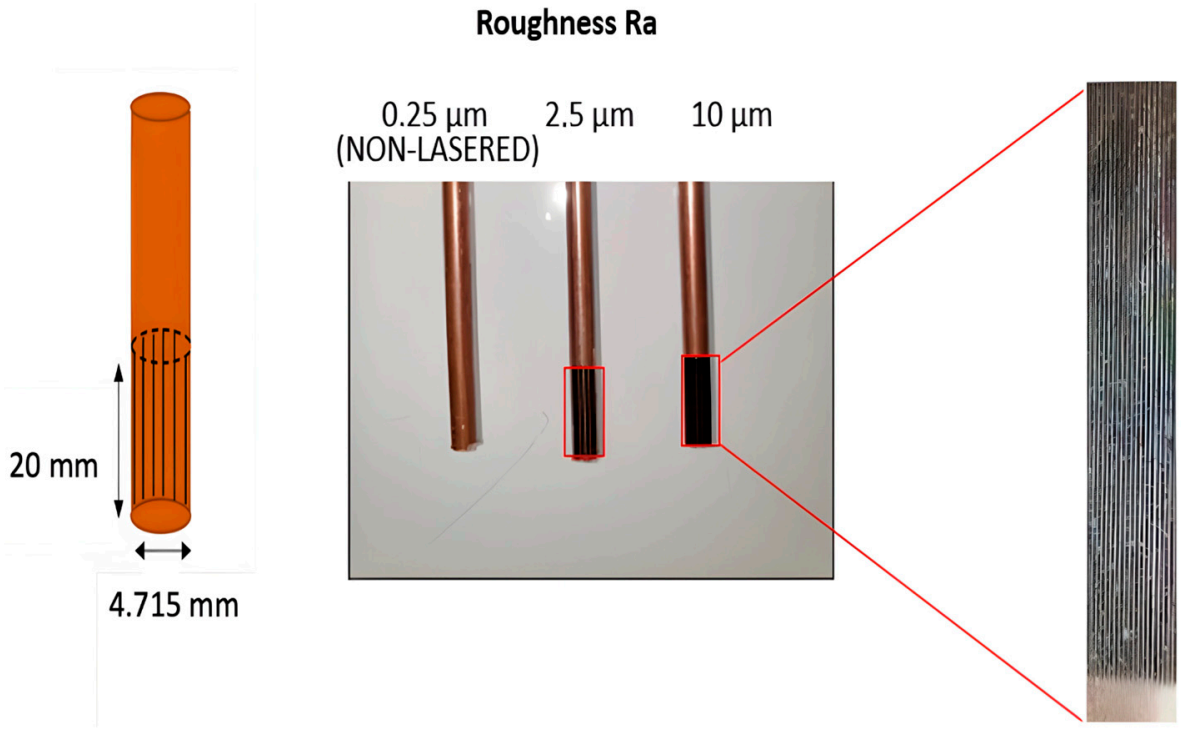

Figure 1. Scheme of a textured copper cylinder with valleys represented by the continuous dark lines (**left**) and a picture of textured copper cylinders (**right**). (The textured part in the red box was zoomed for better visibility).

Table 1. Designation of Ra roughness values.

	R0 (Nontextured)	R1	R2	R3
Ra (µm)	0.26 ± 0.05	0.5 ± 0.1	5 ± 0.1	10 ± 0.05

2.3. Coating Process

The coating procedure involves immersing the preheated copper cylinder into the PA11 powder whose particles are suspended via rising air flow. In contact with the hot metal, the PA11 powder melts onto the metal surface and a thin thermoplastic coating forms (Figure 2). For this, the PA11 powder was fluidized in a 200 mm diameter and 400 mm height hopper crossed by an air flow. Copper specimens were preheated to 270, 300 and 320 °C to effectively melt the PA11 powder [23] and to assess the impact of the substrate temperature on coating properties. The time of immersion in the fluidized bed was chosen from the best process parameters found in our previous work of 6 s [20]. The coating length measured 20 mm.

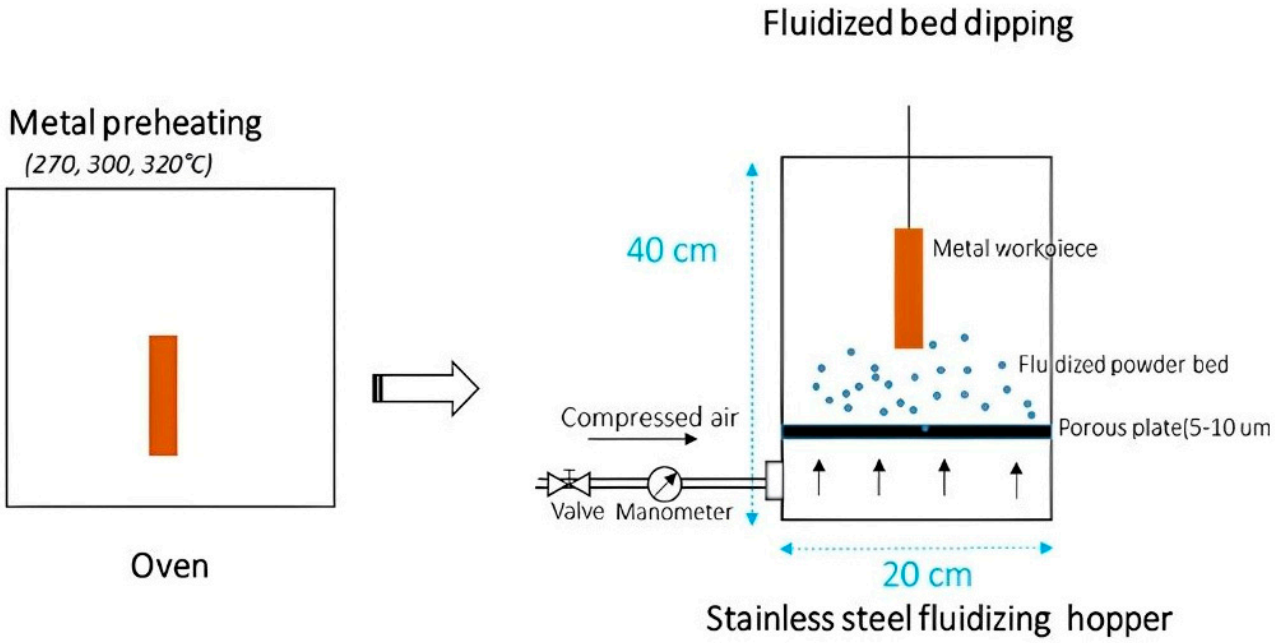

Figure 2. Scheme of the coating process [20].

2.4. Sterilization Process

The samples were sterilized through a physical method according to the standard ISO 17665-1:2006 [24]. For this, they were placed in a 6 L autoclave under a steam pressure of 1.8 bar for 20 min at 121 °C. Temperature conditions were monitored thanks to K-type thermocouples. Then, they were oven-dried at 80 °C for 24 h to remove any remaining water.

2.5. Adhesion Strength Test

To assess the adhesion of PA11 coating on copper cylinders, peel tests were conducted. These tests involved removing the coating from copper substrates. For this purpose, an MTS tensile test device was employed with a 1 kN load cell, operating at 6 mm·min^{-1}. We used a custom-made scraper to determine the adhesion strength at the interface between the coating and the copper substrate along the copper cylinder (Figure 3). More details on the mechanical test are given in our previous paper [20]. We performed tests on five replicate specimens of each material to ensure reliability.

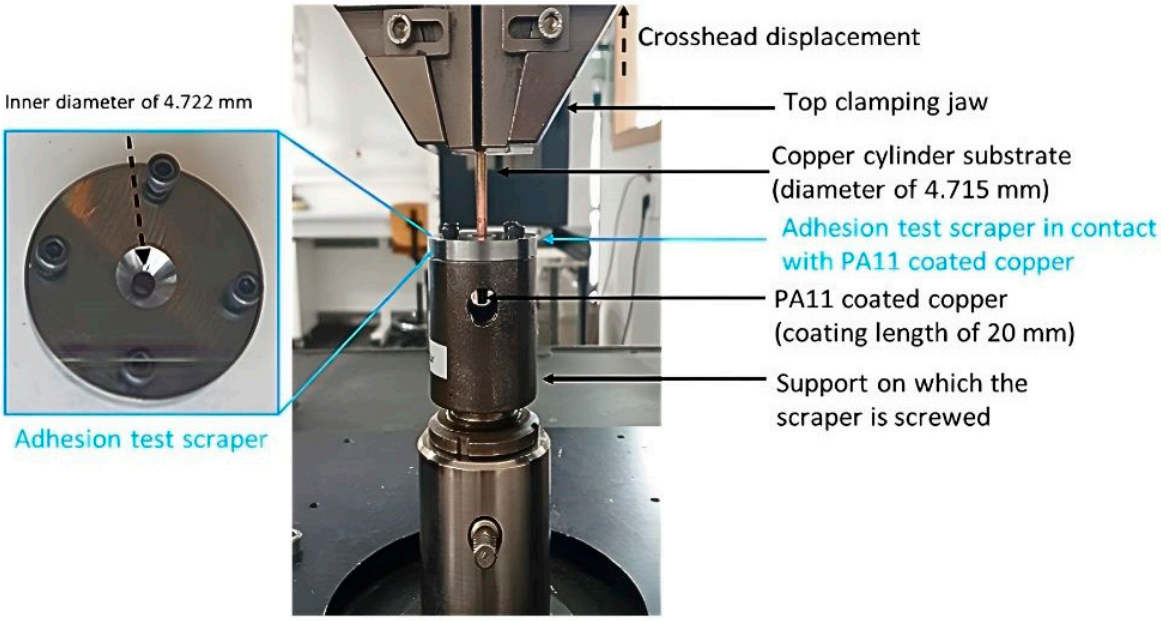

Figure 3. Picture of the mechanical test bench [20].

To quantify the interfacial adhesion strength, we first measured the force F required to remove the peeled-off coating from samples treated at temperatures of 270 °C, 300 °C and 320 °C. The strength, denoted as S, can be calculated as follows:

$$S = \frac{F}{A} \tag{2}$$

where F is the force required to peel off the coating (n) and A is the cross-sectional area (mm^2). A was determined as follows:

$$A_{(T(°C))} = 2\pi \times r \times d_{T(°C)} = 2\pi \times 2.36 \times d_{T(°C)} \tag{3}$$

where r represents the constant inner radius of the coating (r = 2.36 mm) and $d_{T(°C)}$ represents the length of the coating part (mm) peeled off due to the maximum force recorded at low displacement of the scraper.

2.6. Surface Morphology Analysis

After the peeling test, the surface morphology of the Torn Polyamide Coating (TPC) that was in contact with the copper substrate was observed with scanning electron microscopy (SEM), using the HIROX SH-3000 (Hirox Europe, Limonest, France), to monitor the impact of the processing, texturing and sterilization on the coating/metal interface debonding mechanisms. The face that was analyzed was metallized using gold at 30 mA for 60 s (desk V, Denton Vacuum, Moorestown, NJ, USA). The accelerated voltage was adjusted to 25 kV.

2.7. Surface Chemical Analysis

2.7.1. X-ray Photoelectron Spectrometry

X-ray photoelectron spectra of TPC were collected thanks to a Thermo K-alpha spectrometer. The samples were irradiated with a monochromatic source (Al Kα, 1486.6 eV) under vacuum with a pressure of 1×10^{-9} mbar. The pass energy was set to 20 eV. During the analysis, a dual beam charge neutralization system was employed to counteract any charge effects that occurred. This system used both low energy electrons and Ar^+ ions, providing a unique capability to consistently neutralize charges throughout the process. The energy calibration of all spectra was accomplished using the binding energy of a carbon

1 s orbital at 285.0 eV. For details related to the mathematical fitting, please refer to our previous publication [20].

2.7.2. Fourier Transform Infrared Spectroscopy Analysis

The functional groups that could witness the eventual thermo-oxidation of PA11 due to the sterilization step were monitored with a Perkin Elmer spectrometer. The equipment was outfitted with a single-reflection diamond ATR. The inner faces of the TPC were analyzed, and the spectra were recorded from the average of 32 scans in the 650 to 4000 cm^{-1} spectral range with a resolution of 2 cm^{-1}. Normalization of the spectra was performed using the 2925 cm^{-1} reference band which is associated with the CH_2 methylene groups.

2.7.3. Auger Spectroscopy Analysis

Auger analyses were carried out with a JEOL LAMP 9500F Auger spectrometer (JEOL Ltd., Tokyo, Japan) working under UHV conditions (<2 $\times$ 10^{-7} Pa). The UHV equipment was a Schottky Field Emission Auger Electron Spectrometer (FE-AES) dedicated to a very high electron probe spatial resolution analysis and high brightness. The HSA analyzer (Hemi-Spherical electron Analyzer) coupled with a multichannel detector (7 channeltrons) offer ideal settings for energy-resolved Auger analysis. Large kinetic energy (KE) AES spectra (from 0 to 2500 eV) were recorded with DE/E = 0.5%, as a large KE range in the Auger process probability is greater than the radiative de-excitation phenomenon. AES experiments were performed onto focused areas (few nm^2) or along few nm to hundred nm (line scan mode).

2.8. Tensile Tests on Nonsterilized and Sterilized Films

In order to prepare the film for tensile tests, PA11 powder has been dried at 80 °C for 24 h and then placed in the heating press at 210 °C for 5 min without pressure to reach the melted state and then under 10 bar pressure for the same time. A nonstick coating was previously placed on each side of the powder to obtain a good surface quality on the film. The thickness of these films is comparable to that of the coating obtained with fluidized bed dipping, i.e., about 500 microns. The sterilization process applied on these films is the same as that applied to the coating obtained with fluidized bed dipping, i.e., 1.8 bar for 20 min at 121 °C. Samples have been punched into the film in order to obtain the classical dog bone shape with an overall length of 7.5 cm, a central part of 4 mm of width and a linear central part of 3 cm. A pneumatic clamping jaw monitor with an air pressure fixed at 5 bars is used to hold the sample in the 12 mm wide part on the MTS tensile test machine connected to a 1 kN load cell. The strain rate was set at 50 mm·min^{-1}. We performed five tensile tests on the sterilized and nonsterilized films to evaluate an average behavior as well as a significant error for our data.

3. Results and Discussion

3.1. Impact of the Texturing on the Adhesion Strength and the Steam Sterilization

Firstly, the adhesion strength of nontextured and textured samples before sterilization was determined. For this purpose, the force needed to tear out the PA11 coating was recorded as the scraper runs along the copper substrate which was preheated to 270 °C, 300 °C and 320 °C before the coating process (Figure 4). The mechanical profile did not vary according to the average arithmetic roughness, Ra, from 0.26 µm to 10 µm at 270 °C and 300 °C. Indeed, for all these materials, we notice a first maximal force peak (zone 1 represented by 1 in Figure 4) corresponding to the force needed to only take off a small upper part of the coating, with the lower part of the coating clinging to the copper substrate [20]. This first peak was followed by a second, sharper peak (zone 2) representing the folding of the unstuck upper part and a constant force area (zone 3) representing the simultaneous solicitation of the flexible coating and unfolding of the coating. These results were detailed in a previous work [20].

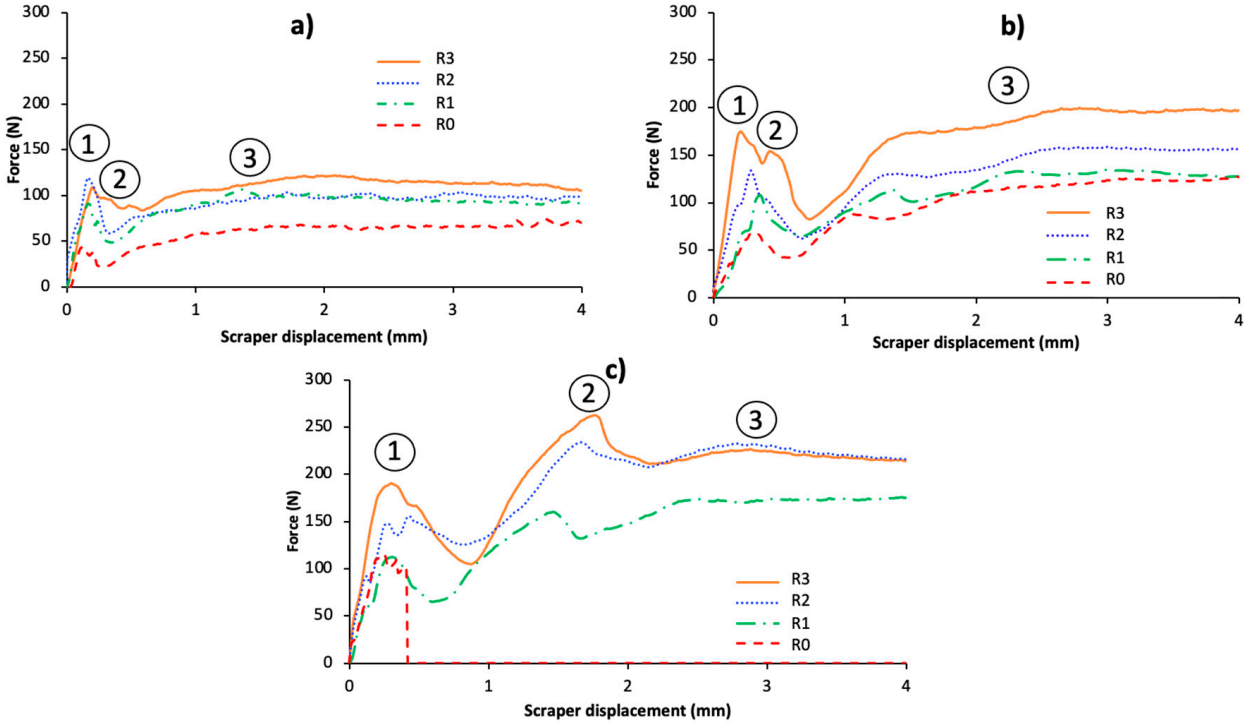

Figure 4. Force versus scraper displacement curves of nonsterilized PA11 coatings whose copper substrates were preheated to 270 °C (**a**), 300 °C (**b**) and 320 °C (**c**) (zone1: first maximal force required to remove the small upper part of the coating; zone 2: second maximal force corresponding to the binding of this upper coating part; zone 3: constant force corresponding to the progressive unfolding of the lower part of the coating).

However, a sharp difference was clearly identified between nontextured and textured copper substrates subjected to the highest preheating temperature (320 °C) (Figure 4). Indeed, we can observe that the force fell to 0 after 0.4 mm of scraper displacement before engraving. This means that the complete coating was removed from the nontextured copper substrates witnessing a very poor anchoring. This fact was developed in our previous paper and was explained with the copper oxide layer that formed on the surface limiting the interfacial adhesion [20]. Nevertheless, textured samples present greater results since the engraving allows for the maintenance of the coating on the substrate surface despite the severe preheating conditions (T = 320 °C). Thus, the roughness parameter strongly influenced the adhesion for the highest preheating temperature and favored the adhesion of the thermoplastic on the metal part during the coating process. This can be easily explained by the higher surface area of the copper support that is in contact with the polyamide coating allowing a higher quantity of thermoplastic to melt onto the metal surface during processing.

Also, to assess the impact of the copper texturing on the quantitative data, the adhesion strengths of the samples were recorded in Table 2. It can be observed that, whatever the preheating temperature, the strength notably increased after texturing. However, we notice only an unsubstantial increase of the adhesion strength with the increase of the Ra parameter (from R1 to R3) induced with the femtosecond laser. This means that the increasing depth of valleys produced with the laser on the substrate did not favor the anchoring of the thermoplastic on the metal. Thus, we suppose that the regularity of the metal surface induced with the engraving procedure mainly favored the adhesion performance rather than the depth of the regular linear troughs. SEM analyses presented later will allow for the verification of our hypotheses and will deepen the discussion.

Table 2. Adhesion strength (MPa) of raw and textured samples before (BS) and after sterilization (AS).

	270 °C		300 °C		320 °C	
	BS	**AS**	**BS**	**AS**	**BS**	**AS**
R0	9.9 ± 0.9	0.21 ± 0.2	3.5 ± 0.5	0.36 ± 0.05	0.38 ± 0.1	0.31 ± 0.1
R1	15.2 ± 0.7	12.5 ± 0.7	4.6 ± 0.5	0.45 ± 0.2	4.29 ± 0.9	0.42 ± 0.1
R2	16.7 ± 1.2	12.8 ± 0.5	5.33 ± 0.5	0.38 ± 0.1	4.63 ± 0.7	0.40 ± 0.2
R3	17.9 ± 0.2	13.2 ± 0.4	6.93 ± 0.4	5.74 ± 1.2	5.63 ± 1.7	4.20 ± 0.6

Then, the influence of the sterilization treatment was assessed for all nontextured and textured samples (Figure 5). We noticed that the sterilization procedure strongly affects the adhesion before texturing (R0) since all coating samples completely came off the copper surface after sterilization, regardless of the preheating temperature (backgrounds of graphics showing a complete debonding after sterilization (force falling to 0) have been grayed out to highlight that these materials are not validated because of a too-weak coating adhesion). However, doubling the parameter Ra (from 0.26 µm to 0.5 µm) had a beneficial impact on the 270 °C-treated specimens. Indeed, it recovered the mechanical behavior, and the adhesion strength is in the same order of magnitude as the nonsterilized one, meaning 70% to 80% of the original value (Table 2). However, it is noted that the strength remains slightly lower than the nonsterilized one. The same trends are observed for R2 and R3. Indeed, even if forces F are quite equivalent before and after sterilization, the length of the upper part of the coating that took off from the copper part was higher after sterilization. Therefore, this led to a lower strength of adhesion *S* (see Equation (2)). This means that a higher quantity of coating was stripped from the copper surface with the same force. A complementary morphology analysis of this upper part torn from the copper surface is needed to bring insights on these results.

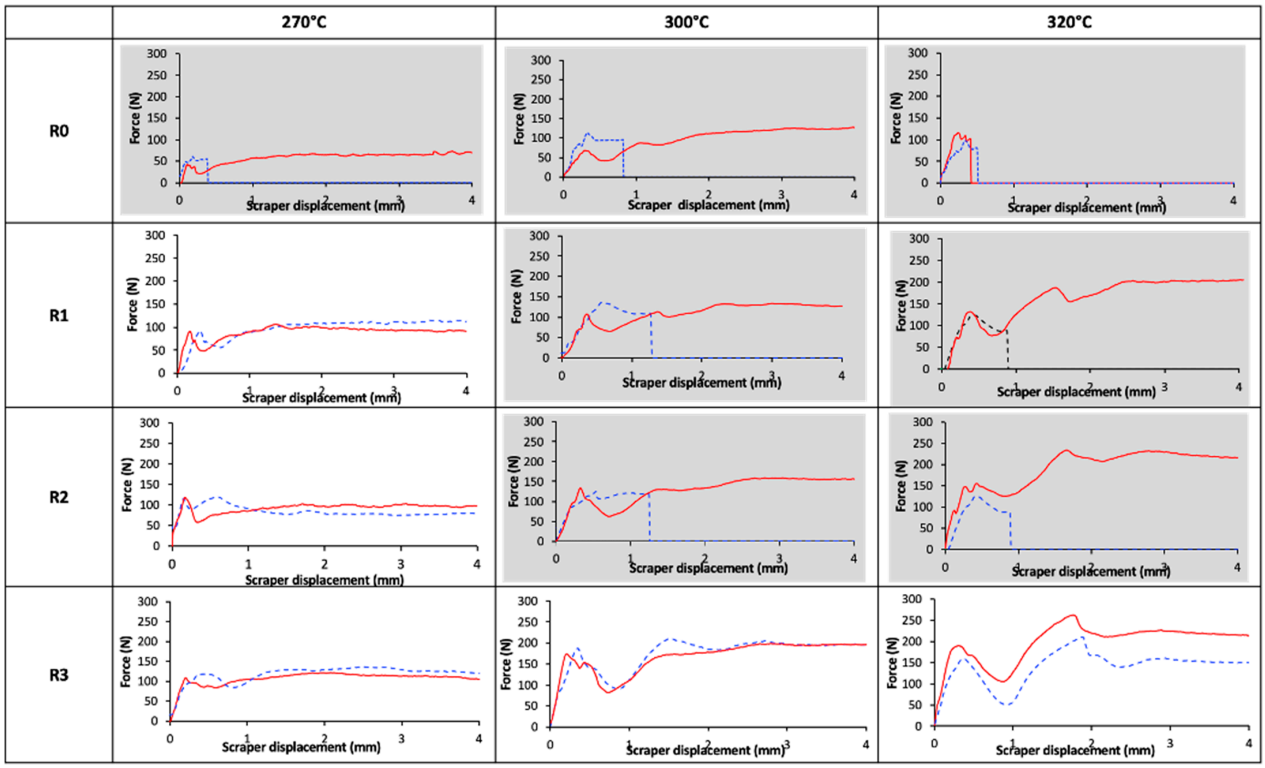

Figure 5. Force versus scraper displacement curves of raw and textured PA11 coatings before (continuous red line) and after (dot blue line) sterilization.

For sterilized samples obtained after preheating at 300 °C and 320 °C, only the 10 µm engraving (R3) allowed for the recovery of the properties comparable to those of nonsterilized ones. Indeed, the retaining percentage of the original value (i.e., before sterilization) soared from 9% for R1 to 82% for R3 at 300 °C and 10% for R1 to 75% for R3 at 320 °C (Table 2).

3.2. Impact of the Steam Sterilization and the Texturing on the Surface Morphology of Peeled Samples

SEM images of the coating surface whose side was in contact with the copper substrate were taken (Figure 6). Firstly, we can easily identify regular domes formed after texturing, corresponding to the polymer having melted into valleys of the textured copper surface during the coating process. In a previous study, we deduced a presence of inorganic matter witnessed via the presence of lighter irregular plates on the coating surface increasing with the preheating temperature (R0) [20]. This tendency is confirmed regardless of the roughness value induced with the laser during the texturing of the copper cylinders. SEM coupled with Auger spectroscopy analysis allowed us to attribute these relief plates to copper-based species (see Appendix A). This presence of copper oxide caused by the harsh conditions of the copper preheating explains the lower mechanical properties for the highest preheating temperature for the same Ra value.

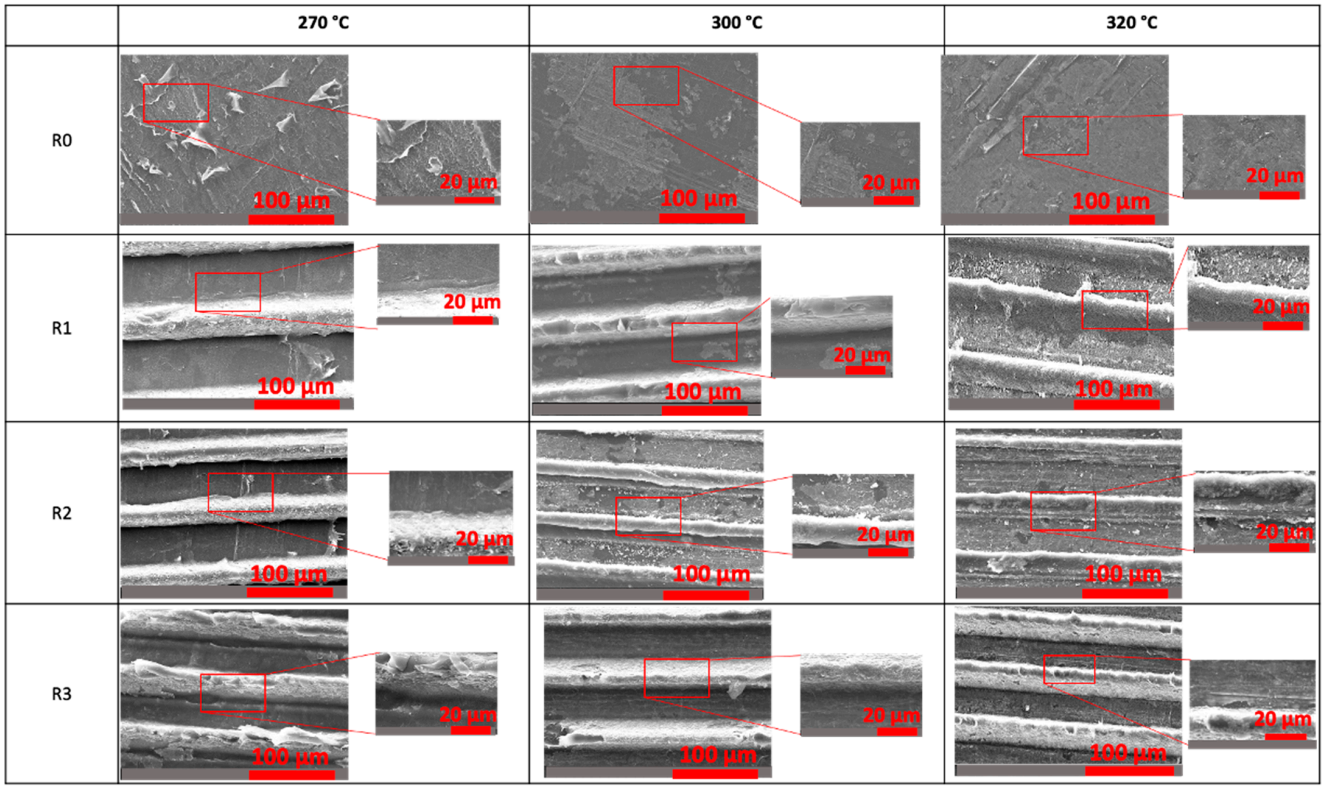

Figure 6. SEM images of PA11 samples detached from raw and textured copper substrates before sterilization (preheating temperatures of copper: 270 °C, 300 °C and 320 °C).

After sterilization, the domes of coatings presented a different aspect (Figure 7). Indeed, nonregular, lace-like structures along the thermoplastic domes were observed. Therefore, we verified if the sterilization had damaged the chemical composition of the coating polymer. For this purpose, Fourier transform infrared spectroscopy (FTIR) analyses were performed on this coating side. Results are presented in the Appendix A. No difference was found between the peaks assigned to polyamide 11 band vibrations in the spectra before and after sterilization, evidencing that the steam sterilization had no notable effect on the chemical composition of the thermoplastic. Also, mechanical properties of nonsterilized

and sterilized PA11 were assessed by evaluating the tensile properties of PA11 films processed at the laboratory from the same PA11 powder used to carry out the coatings (see Section 2.8). As reported in Appendix A (Appendix A.3), no significant change on tensile properties was deduced from mechanical tests on PA11 films. Thus, we can suggest that only rheological properties of the polyamide 11 were changed in the sterilization process, the polymer has been stretched under steam and these changes were responsible for these physical modifications. Also, as for nonsterilized samples, lighter irregular plates attributed to copper-based species were observed. In addition, to understand the changes in the mechanical performance after sterilization, X-ray photoelectron spectrometry was performed.

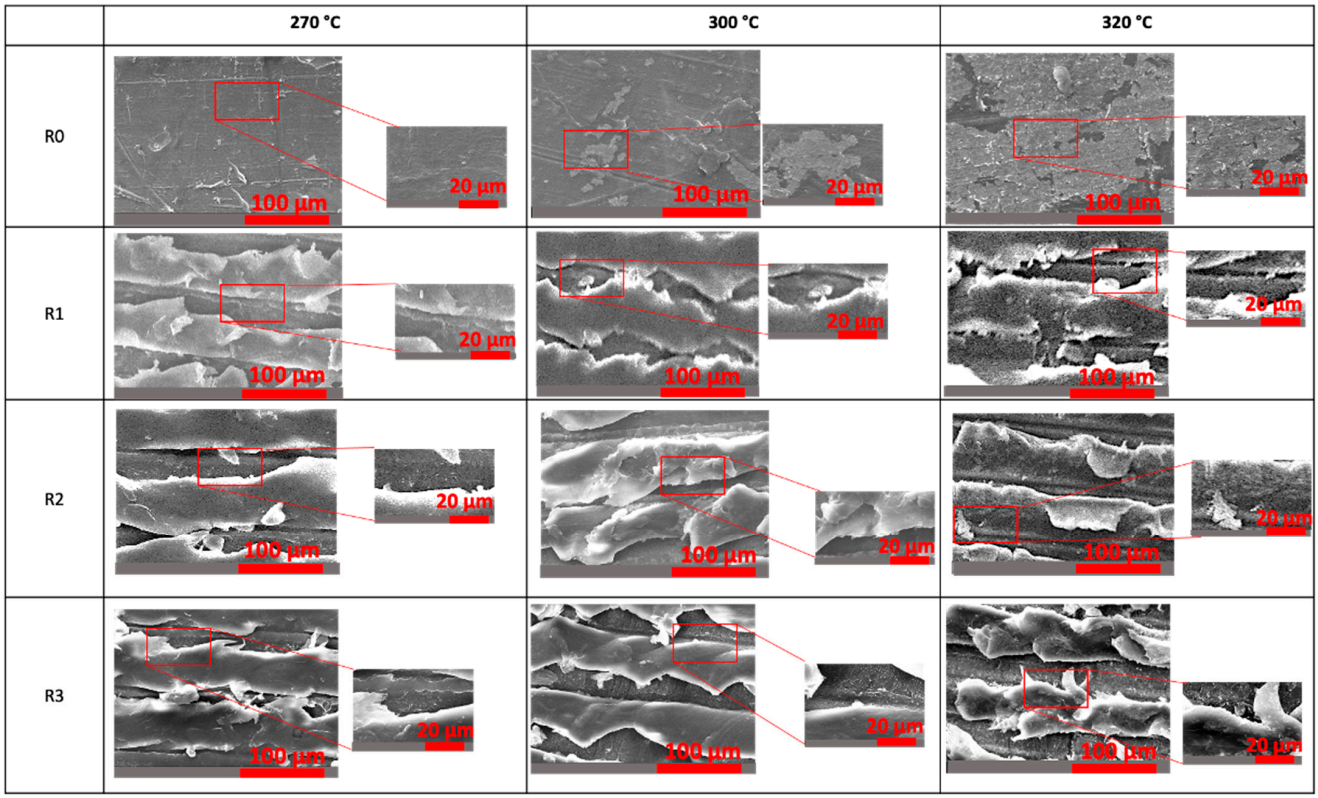

Figure 7. SEM images of PA11 samples detached from raw and textured copper substrates after sterilization (preheating temperatures of copper: 270 °C, 300 °C and 320 °C).

3.3. Impact of the Steam Sterilization and the Texturing on the Chemical Properties of Peeled Samples

XPS was carried out on the coating surface whose side was in contact with the copper substrate for R0 and R3 samples before (NS) and after (S) sterilization. The atomic percentages of the elements C, attributed to the presence of the organic matter (here the coating polymer PA11), and Cu, attributed to copper present at the surface of the coating samples, were deduced from the normalization and the fitting treatments with the software CasaXPS (vers. 2.3.24) (Table 3). The ratio $\frac{at\%Cu}{at\%C}$ easily highlighted that the sterilization gave rise to an increase of the copper rate on the thermoplastic coatings torn from the copper substrates. This suggests that the steam affected the stability of the copper cylinders whose small surface part (copper oxide) remained stuck to the polymer after the mechanical test.

Figure 8 depicts the contribution of copper-based species present on the analyzed coating samples that were deduced from the XPS spectra. Before sterilization, copper-based species were found under two forms, copper (I) oxide Cu_2O and copper (II) hydroxide $Cu(OH)_2$, that were clearly identified for all untextured and textured samples (R0 and R3) except from nonsterilized samples whose copper was preheated to 270 °C (at the left of

Figure 8). The presence of these species is due to the severe preheating conditions carried out at 300 °C and 320 °C having oxidized the metal. Then, after sterilization, Cu_2O and $Cu(OH)_2$ are present at the coating surface regardless of the preheating temperature (even at 270 °C). This suggests that the sterilization caused the oxidation of the metal surface. In addition, we noticed that the rate of $Cu(OH)_2$ particularly increased after sterilization. As proposed in our previous study, the formation of copper (II) hydroxide can result from copper (I) oxide in the presence of water and oxygen [20]. Hence, the steam formed during sterilization has certainly contributed to the formation of copper hydroxide. However, the presence of this copper oxide after sterilization did not affect the interfacial adhesion between the coating and the metal substrate presenting the highest Ra value (R3). Indeed, as seen previously, the 10 µm engraving (R3) of the copper substrate generated mechanical performance (adhesion strength) comparable to those of nonsterilized ones.

Table 3. Chemical composition (at%: atomic percentage) of the surface of peeled-off nonsterilized (NS) and sterilized (S) coating samples in the binding energy range 0–1400 eV.

	270 °C			300 °C			320 °C		
	at%C	**at%Cu**	$\frac{\text{at\%Cu}}{\text{at\%C}}$	**at%C**	**at%Cu**	$\frac{\text{at\%Cu}}{\text{at\%C}}$	**at%C**	**at%Cu**	$\frac{\text{at\%Cu}}{\text{at\%C}}$
NS-R0	80.2	-	-	73.9	0.1	0.001	75	0.4	0.005
S-R0	81	0.6	0.01	66.8	3.4	0.05	74.9	3.4	0.05
NS-R3	81.4	-	-	79	0.2	0.002	73.2	0.2	0.003
S-R3	82.4	1.1	0.01	82.5	1.4	0.02	84.7	1.6	0.02

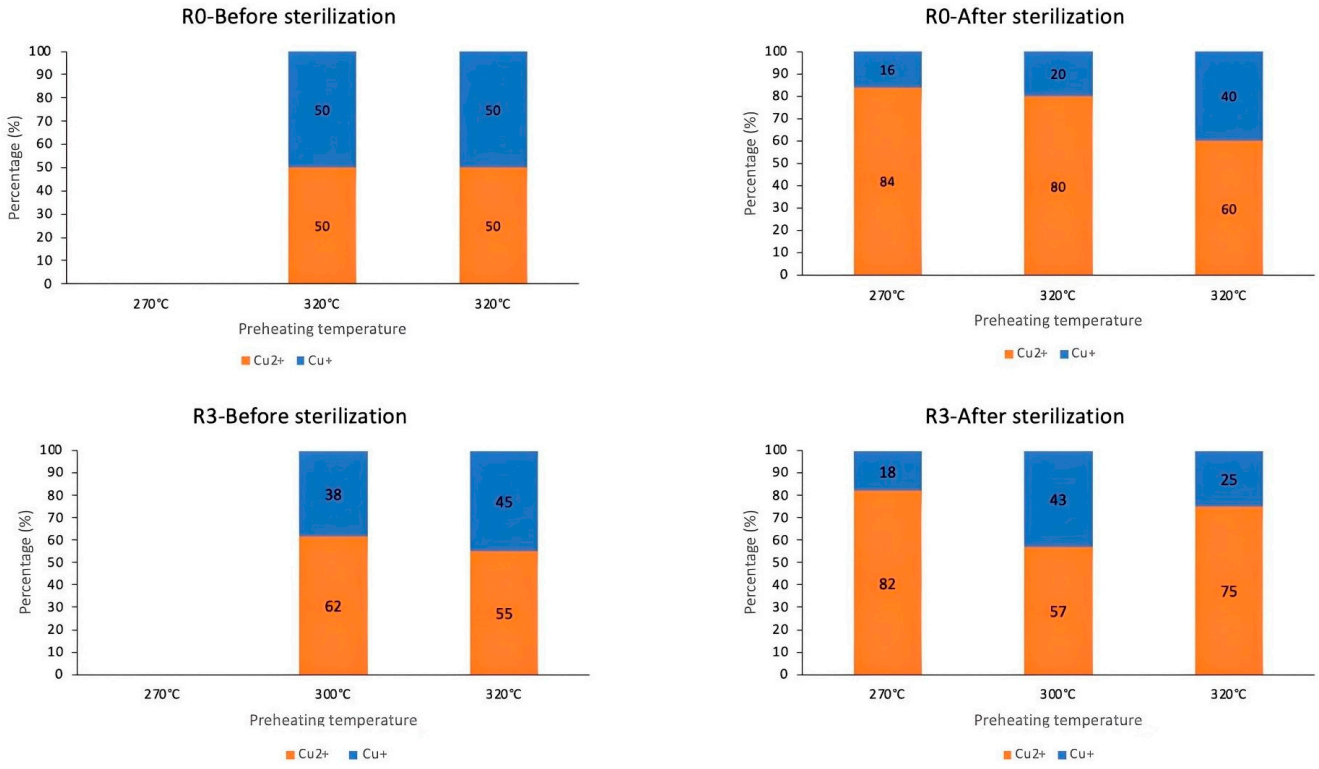

Figure 8. Rates of Cu^{2+} (under $Cu(OH)_2$ form) and Cu^{+} (under Cu_2O form) species determined via XPS (from Cu 2p spectra) on the surface of peeled-off nonsterilized and sterilized coating samples.

4. Conclusions

This study investigated the impact of steam sterilization of a polyamide-coated copper, single-use device before and after ultrafast laser texturing. A laboratory-made mechanical test was employed to assess the coating adhesion properties. Firstly, the sterilization highly limited the coating adhesion signifying that the conditions of sterilization impacted the

interface. Nevertheless, the texturing enabled the recovery of the adhesion strength thanks to the increasing surface area of the copper substrate. Contrary to materials whose copper substrate was heated at a low temperature (T = 270 °C), a high arithmetic roughness value, Ra, induced via laser surface texturing (LST) was necessary (Ra = 10 µm) to obtain an adhesion strength comparable to the original coating. The analysis of the composition by FTIR of the coating side that was stick to the metal substrate, demonstrated that, even if rheological properties were certainly modified through the sterilization process, witnessed by the lace-like structure of the polyamide visualized on SEM images, its chemical structure has not been disturbed. Thanks to XPS characterization, it was evident that copper's chemical instability to steam sterilization was mainly responsible for the mechanical interfacial properties loss after the sterilization.

In order to improve the adhesion properties, a biocompatible primer could enhance the adhesion resistance to the sterilization process. Otherwise, cytotoxicity and sterility tests should be brought to ensure that the medical device can be effectively used for surgical procedures.

Author Contributions: Conceptualization, C.B. and F.L.; Validation, C.B., A.A. and J.-C.D.; Writing—original draft, C.B. and F.L.; Visualization, A.A. and J.-C.D.; Supervision, A.A., J.-C.D. and F.L. All authors have read and agreed to the published version of the manuscript.

Funding: This work was supported by the program POCTEFA EFA313/19 LGMed.

Institutional Review Board Statement: Not applicable.

Informed Consent Statement: Not applicable.

Data Availability Statement: Data are contained within the article.

Acknowledgments: We wanted to thank ARKEMA (Serquigny, France) for providing us with the PA11 powder.

Conflicts of Interest: The authors declare no conflict of interest.

Appendix A

Appendix A.1 Infrared Measurements

The chemical composition of the organic matter on side the that was stuck to the copper substrate was determined (Figure A1).

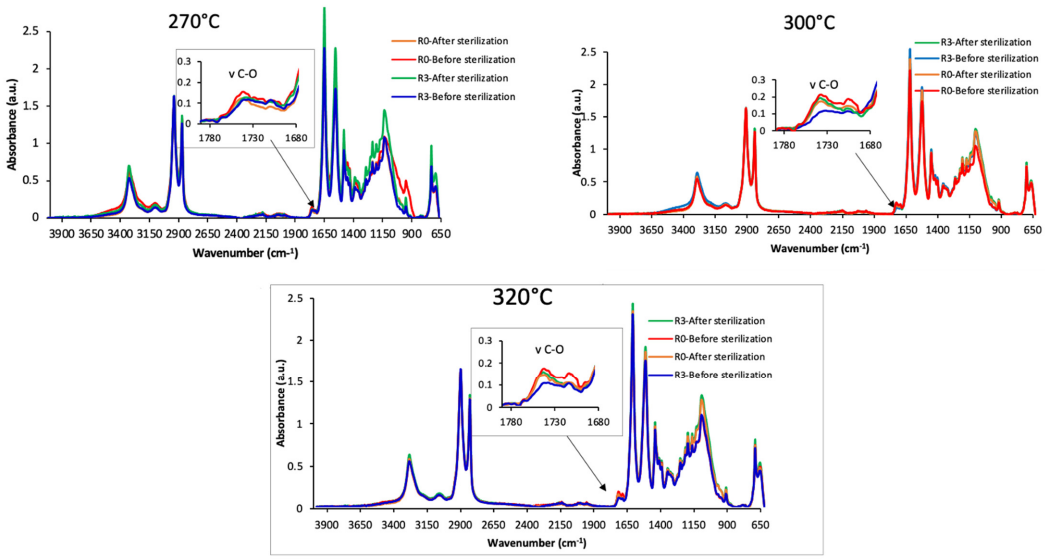

Figure A1. FTIR spectra of PA11 samples detached from raw and textured copper substrates before and after sterilization (preheating temperatures of copper: 270 °C, 300 °C and 320 °C).

Appendix A.2 SEM Coupled with Auger Spectroscopy Measurements

In order to confirm the attribution of the relief plates present on the coatings analyzed with SEM after sterilization, SEM analysis coupled with Auger spectroscopy was carried out on the sterilized 320 °C-pretreated R3 sample. It revealed the presence of copper on the domes of the rows (which is not so evident in the valleys) (Figure A2).

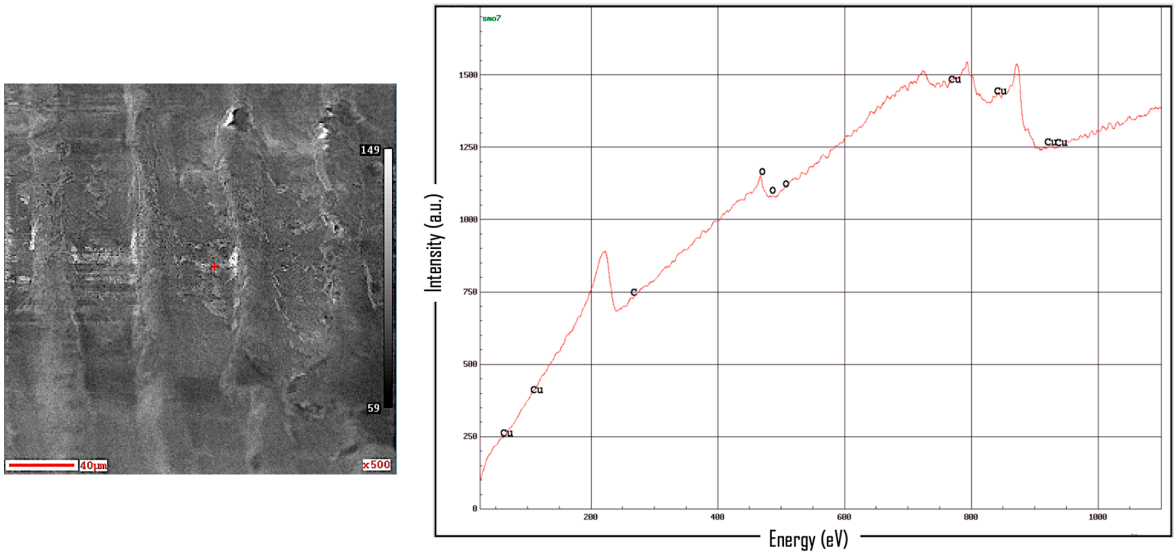

Figure A2. SEM analysis coupled with Auger spectroscopy of a relief plate present on ripped off nonsterilized coating sample (preheating temperature = 320 °C, Ra = 10 µm) (the red point in the figure corresponds to the area analyzed by SEM-Auger spectroscopy (graph at the right)).

Appendix A.3 Tensile Tests on PA11 Films

Figure A3 shows the average behavior of tensile tests on each type of film. One can see that the tensile modulus and the maximum stress are identical, taking into account the experimental error. During these tensile tests, we observe a ductile behavior; it appears that there is a reduction of the central part of the sample after having exceeded the maximum stress. Moreover, from a certain apparent strain value, a plateau is reached at a strain of around 38 MPa whatever the state of the film, either nonsterilized or sterilized. One can therefore conclude that there is no significant effect of the sterilization step on the mechanical behavior of PA11 films, and, therefore, we conclude that there is no effect on the PA11 coating.

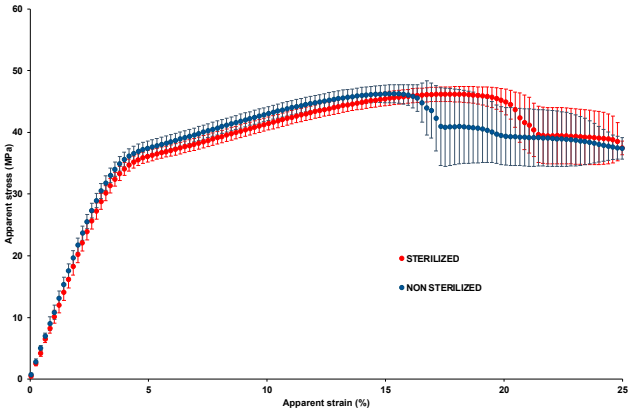

Figure A3. Stress–strain curves before and after sterilization of PA11 films.

References

1. Bolton Surgical Catalogue. Available online: https://www.boltons.co.uk/ (accessed on 16 May 2023).
2. Hyden Medical Instruments. Available online: https://www.haydenmedical.com/product-category/ob-gyn/lletz/non-conductive-instruments/ (accessed on 12 October 2023).
3. Imre, B.; Pukánszky, B. Compatibilization in bio-based and biodegradable polymer blends. *Eur. Polym. J.* **2013**, *49*, 1215–1233. [CrossRef]
4. Human Regulatory: Medical Devices. Available online: https://www.ema.europa.eu/en/human-regulatory/overview/medical-devices (accessed on 3 May 2023).
5. Conformity Assessment Overview. Available online: https://www.tga.gov.au/how-we-regulate/manufacturing/medical-devices/conformity-assessment/conformity-assessment-bodies/tga-conformity-assessment-certification/conformity-assessment-overview (accessed on 5 January 2023).
6. Medical Device Performance Testing. Available online: https://atslab.com/testing-and-analysis-company/medical-device-performance-testing/ (accessed on 16 May 2023).
7. Sassonia, R.C.; Dua, K.; Kikuchi, I.S.; Rediguieri, C.F.; de Jesus Andreoli Pinto, T. Impact of sterilization methods on electrospun scaffolds for tissue engineering. *Eur. Polym. J.* **2016**, *82*, 182–195.
8. Wingham, J.R.; Omran, M.; Shepherd, J.; Majewski, C. Effect of steam autoclaving on laser sintered polyamide 12. *Rapid Prototyp. J.* **2021**, *27*, 45–52. [CrossRef]
9. Told, R.; Ujfalusi, Z.; Pentek, A.; Kerenyi, M.; Banfai, K.; Vizi, A.; Szabo, P.; Melegh, S.; Bovari-Biri, J.; Pongracz, J.E.; et al. A state-of-the-art guide to the sterilization of thermoplastic polymers and resin materials used in the additive manufacturing of medical devices. *Mater. Des.* **2022**, *224*, 111119. [CrossRef]
10. Santoro, F.; Zhao, W.; Joubert, L.M.; Duan, L.; Schnitker, J.; van de Burgt, Y.; Lou, H.Y.; Liu, B.; Salleo, A.; Cui, L.; et al. Revealing the cell-material interface with nanometer resolution by focused ion beam/scanning electron microscopy. *ACS Nano* **2017**, *11*, 8320–8328. [CrossRef] [PubMed]
11. Choi, J.; Chung, M.H.; Dong, K.Y.; Park, E.M.; Ham, D.J.; Park, Y.; Song, I.S.; Pak, J.J.; Ju, B.K. Investigation on fabrication of nanoscale patterns using laser interference lithography. *J. Nanosci. Nanotechnol.* **2011**, *11*, 778–781. [CrossRef] [PubMed]
12. Uhlmann, E.; Schweitzer, L.; Kieburg, H.; Spielvogel, A.; Huth-Herms, K. The effects of laser microtexturing of biomedical grade 5Ti-6Al-4V dental implants (abutment) on biofilm formation. *Procedia CIRP* **2018**, *11*, 184–189. [CrossRef]
13. Shivakoti, I.; Kibria, G.; Cep, R.; Pradhan, B.B.; Sharma, A. Laser surface texturing for biomedical applications: A review. *Coatings* **2021**, *11*, 124. [CrossRef]
14. Moura, C.G.; Pereira, R.; Buciumeanu, M.; Carvalho, O.; Bartolomeu, F.; Nascimento, R.; Silva, F.S. Effect of laser surface texturing on primary stability and surface properties of zirconia implants. *Ceram. Int.* **2017**, *43*, 15227–15236. [CrossRef]
15. Krylach, I.V.; Kudryashov, S.I.; Olekhnovich, R.O.; Moskvin, M.K.; Uspenskaya, M.V. Tuning water wetting angle of a steel surface via nanosecond laser ablative nano/microtexturing for chemical and biomedical microfluidic applications. *Laser Phys. Lett.* **2019**, *16*, 105602. [CrossRef]
16. Selvamani, V.; Zareei, A.; Elkashif, A.; Maruthamuthu, M.K.; Chittiboyina, S.; Delisi, D.; Li, Z.; Cai, L.; Pol, V.G.; Seleem, M.N.; et al. Hierarchical Micro/Mesoporous Copper Structure with Enhanced Antimicrobial Property via Laser Surface Texturing. *Adv. Mater. Interfaces* **2020**, *7*, 1901890. [CrossRef]
17. Razzaq, L.A.; Abdullah, A.Q. Enhancement of the corrosion resistance of copper metal by laser surface treatment. *Iraqi J. Phys.* **2020**, *18*, 13–19.
18. Long, J.; Zhong, M.; Fan, P.; Gong, D.; Zhang, H. Wettability conversion of ultrafast laser structured copper surface. *J. Laser Appl.* **2019**, *27*, S29107. [CrossRef]
19. Conradi, M.; Sever, T.; Gregorčič, P.; Kocijan, A. Short-and long-term wettability evolution and corrosion resistance of uncoated and polymer-coated laser-textured steel surface. *Coatings* **2019**, *9*, 592. [CrossRef]
20. Badji, C.; Allal, A.; Dupin, J.C.; Léonardi, F. Polyamide powder coating of copper substrates: Impact of process parameters on the surface properties, the adhesion strength and the interface microstructure. *Prog. Org. Coat.* **2023**, *174*, 107253. [CrossRef]
21. Ansabere Surgical SL. Available online: https://cordis.europa.eu/project/id/744712 (accessed on 7 February 2022).
22. *ISO 4287*; Geometrical Product Specifications—Surface Texture: Profile Method: Terms, Definitions and Surface Texture Parameters. ISO: Geneva, Switzerland, 1998.
23. Verbelen, L.; Dadbakhsh, S.; Van Den Eynde, M.; Kruth, J.P.; Goderis, B.; Van Puyvelde, P. Characterization of polyamide powders for determination of laser sintering processability. *Eur. Polym. J.* **2016**, *75*, 163–174. [CrossRef]
24. *ISO 17665-1:2006*; Sterilization of Health Care Products. ISO: Geneva, Switzerland, 2006.